Nighttime formation of peroxy and hydroxyl radicals during the BERLIOZ campaign: Observations and modeling studies

Andreas Geyer,^{1,2} Kurt Bächmann,³ Andreas Hofzumahaus,⁴ Frank Holland,⁴ Stefan Konrad,⁴ Thomas Klüpfel,⁵ Hans-Werner Pätz,⁴ Dieter Perner,⁵ Djuro Mihelcic,⁴ Hans-Jürgen Schäfer,⁴ Andreas Volz-Thomas,⁴ and Ulrich Platt¹

Received 22 March 2001; revised 11 July 2001; accepted 1 October 2001; published 23 January 2003.

[1] Traditionally, tropospheric radical chemistry is discussed in terms of the daytime photochemically produced hydroxyl radical (OH). Radicals, however, are also important during nighttime: this is especially true for ozone and the nitrate radical (NO₃), which both act as key initiators of the degradation of alkenes such as biogenic monoterpenes. These reactions lead to the formation of peroxy radicals (HO₂ and RO₂) and hydroxyl radicals at night. We present recent observations of nighttime concentrations of NO₃, RO₂, HO₂, and OH by differential optical absorption spectroscopy (DOAS), matrix isolation electron spin resonance (MIESR), laser-induced fluorescence (LIF), and a chemical amplifier (CA) in the framework of the Berliner Ozonexperiment (BERLIOZ) campaign at Pabstthum, Germany, together with modeling studies of nocturnal radical chemistry. Modeled RO₂ mixing ratios reached 40 ppt while the measured RO_x level went up to 22 ppt at the same time. Modeled and measured HO₂ mixing ratios were up to 6 and 4 ppt, respectively. In the case of OH, a nocturnal concentration of $(1.85 \pm 0.82) \times 10^5$ cm⁻³ was measured during one night. At this time, the model yielded an OH level of $(4.1 \pm 0.7) \times 10^5$ cm⁻³. This overestimation by the model could point to a missing nocturnal sink of OH. Nitrate radical reactions with terpenes were found responsible for producing 77% of the RO₂ radicals, 53% of the HO₂, and 36% of the OH radicals during night. Nighttime ozonolysis formed 12% of the RO₂, 47% of the HO₂, and 64% of the OH radicals. Another 11% of the RO₂ radicals were formed by OH-volatile organic compound (VOC) reactions. A positive linear correlation of RO₂ and NO₃ was observed and could be reproduced in model calculations originating from the loss of both radicals by reaction with NO and the NO₃-initiated RO₂ production. The contribution of nighttime OH to the atmosphere's oxidation capacity (oxidation rate of VOCs, CO, and CH₄) was found negligible (<0.5%). INDEX TERMS: 0365 Atmospheric Composition and Structure: Troposphere—composition and chemistry; 0322 Atmospheric Composition and Structure: Constituent sources and sinks; 0345 Atmospheric Composition and Structure: Pollution—urban and regional (0305); KEYWORDS: nighttime chemistry, NO₃, peroxy radicals, OH, ozonolysis

Citation: Geyer, A., et al., Nighttime formation of peroxy and hydroxyl radicals during the BERLIOZ campaign: Observations and modeling studies, *J. Geophys. Res.*, 108(D4), 8249, doi:10.1029/2001JD000656, 2003.

1. Introduction

[2] Large amounts of nitrogen oxides (NO_x) and volatile organic compounds (VOCs) are emitted into the atmosphere

Copyright 2003 by the American Geophysical Union. 0148-0227/03/2001JD000656

by human and natural activities (see recent reviews by Guenther et al. [2000]; Placet et al. [2000]; Sawyer et al. [2000]). In the planetary boundary layer NO_x and VOCs are to a small extent directly removed by wet and dry deposition [Wesley and Hicks, 2000; Jacob, 2000] or to a major part transformed by reaction with free radicals such as hydroxyl (OH) radicals, nitrate (NO_3) radicals, and ozone (O_3) [e.g., Atkinson, 2000].

[3] Sources of hydroxyl radicals during daytime are the photolysis of ozone, of nitrous acid and of aldehydes [e.g., *Platt et al.*, 1986; *Alicke et al.*, 2003]. In rural areas the ozonolysis of alkenes can also be an important OH source [*Paulson and Orlando*, 1996; *Ariya et al.*, 2000]. These formation paths lead to daytime OH levels in the range of several 10⁶ cm⁻³ [e.g., *Hein et al.*, 1997; *Holland et al.*,

¹Institut für Umweltphysik, Universität Heidelberg, Heidelberg, Germany.

²Now at Department of Atmospheric Sciences, University of California, Los Angeles, California, USA.

³Institut für Anorganische Chemie, TH Darmstadt, Darmstadt, Germany.

⁴Institut für Atmosphärische Chemie, Forschungszentrum Jülich, Jülich, Germany.

⁵Max-Planck-Institut für Chemie, Mainz, Germany.

1998, 2003]. Due to missing photolysis, nighttime levels of OH radicals are much lower [e.g., *Eisele et al.*, 1996]. The sole source of nitrate radicals is the slow reaction of NO₂ with ozone [*Platt et al.*, 1981]. Nitrate radicals are, however, rapidly destroyed by sunlight so that NO₃ only can accumulate during nighttime up to mixing ratios of some ppt [*Geyer et al.*, 2001].

- [4] Because of these properties hydroxyl radicals are generally ignored during nighttime while nitrate radicals are disregarded during daytime. Recently, however, first evidence was found for an important NO₃ daytime chemistry in the case of the gas-phase oxidation of phenolic aromatic hydrocarbons [A. Geyer et al., Direct observation of daytime NO₃: Implications for urban boundary layer chemistry, submitted to Journal of Geophysical Research, 2002; Kurtenbach et al., 2002]. On the other side the initial attack of NO₃ on a VOC is a potential source of peroxy radicals (RO₂) and HO₂) and OH radicals during night [*Platt et al.*, 1990; Wayne et al., 1991; Canosa-Mas et al., 1992; Jensen et al., 1992; Le Bras et al., 1993; Mihelcic et al., 1993; Benter et al., 1994; Carslaw et al., 1997; Bey et al., 2001]. Another nighttime source of RO_x radicals ($RO_x = RO_2 + HO_2 + OH$) is the ozonolysis of VOCs [e.g., Paulson and Orlando, 1996; Ariya et al., 2000]. The nonphotochemical formation of hydroxyl radicals is thought to initiate the nighttime removal of a large number of VOCs thus increasing the atmospheric oxidation capacity. Peroxy radicals are important chain carriers in the oxidation of hydrocarbons, intermediates in tropospheric ozone generation and precursors for nighttime OH. In addition self-reactions of peroxy radicals are the most important gas-phase source of peroxides in the atmosphere.
- [5] In this paper we report simultaneous observations of NO₃, RO₂, HO₂, and OH together with a large set of ancillary measurements, which were performed in July/August 1998 at the Berliner Ozonexperiment (BERLIOZ) site Pabstthum during several nights. A box model for nighttime radical chemistry (NO₃-O₃-RO_x) was developed to reproduce the observed nocturnal concentrations of RO_x radicals and to study the importance of NO₃ and ozone for the production of RO_x radicals during night.

2. Nighttime RO_x Chemistry

- [6] A schematic diagram of the nighttime NO₃-RO_x chemistry is shown in Figure 1. The chemistry of the nitrate radical in the atmosphere has been explained in detail by different authors [e.g., *Platt et al.*, 1981; *Heikes and Thompson*, 1983; *Wayne et al.*, 1991; *Heintz et al.*, 1996; *Geyer et al.*, 2001]. Nitrate radicals are produced by the reaction of NO₂ with ozone. Equilibrium among NO₃, NO₂, and N₂O₅ is established within a few minutes. In the nocturnal continental boundary layer NO₃ is removed either by (1) N₂O₅ hydrolysis on aerosols, (2) the fast reaction of NO₃ with NO (close to sources of NO_x like road traffic), and (3) by reactions with unsaturated VOCs, especially biogenic monoterpenes [e.g., *Atkinson*, 1997; *Martinez et al.*, 1999; *Gölz et al.*, 2001; *Geyer et al.*, 2001]. Beside this there are a number of other reactions of NO₃, e.g., with RO₂ and HO₂ (Figure 1).
- [7] The reactions of NO_3 with VOCs do not only constitute a major sink of NO_3 but also lead to the formation of RO_x radicals during night: The initial step of these reactions is the addition of NO_3 to a double bond forming a radical

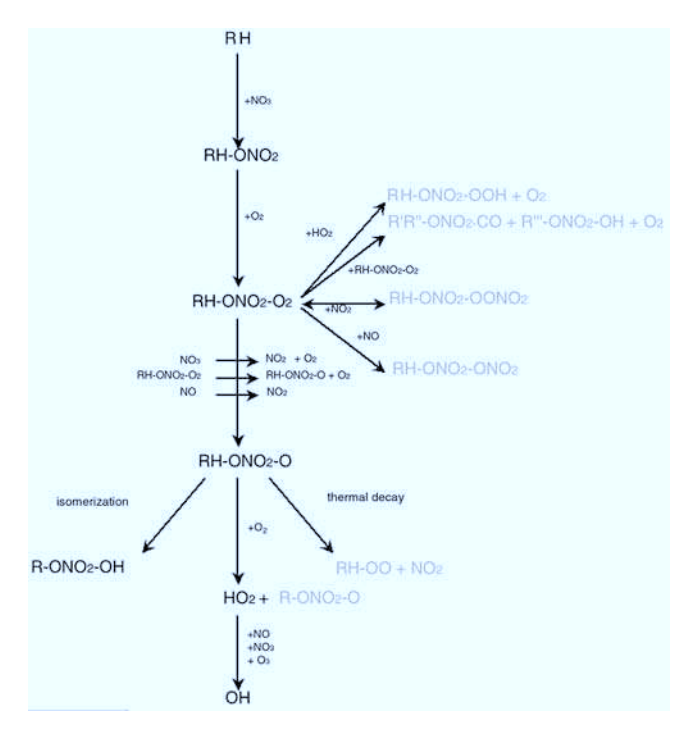


Figure 1. Simplified scheme of the degradation of a VOC (RH) following the attack of a nitrate radical. This oxidation chain can produce peroxy radicals (RH-ONO₂-O₂ and HO₂) and OH radicals during night.

adduct intermediate. The resulting nitratoalkyl radical (Figure 1) rapidly reacts with oxygen forming a nitratoalkyl-peroxy radical (RH-ONO₂-O₂):

$$NO_3 + > C = C < -\frac{O_2}{-} \rightarrow > C(ONO_2) - C(OO) <$$
 (1)

- [8] There exist several reaction pathways for peroxy radicals producing either nitratoalkoxy radicals (RH-ONO₂-O) or a number of stable products (Figure 1). Peroxy radicals rapidly react with NO forming alkoxy radicals. Alternatively is the combination of NO and the peroxy radical yielding dinitrates (RH-ONO2-ONO2), which are a stable product of the peroxy radical degradation mechanism. Organic peroxy radicals also react with the nitrogen oxides NO₂ and NO₃ or undergo self-reaction. Reactions with NO₂ usually establish a steady state with peroxy dinitrates. Another important path is the reaction of peroxy radicals with NO₃. Reactions of peroxy radicals with HO₂ are known to be important sinks for both species and they constitute the only known source for hydrogen peroxide H_2O_2 (if the peroxy radical is HO_2) and hydro peroxides R'-OOH in the atmosphere. These reactions break the peroxy radical degradation chain because hydro peroxides are stable products in the atmosphere at least during night, when photolysis can be neglected. For self-reactions usually two reaction paths were found: (1) the formation of alkoxy radicals R'O (in the case of peroxy radicals formed by NO₃-VOC reactions RH-ONO₂-O) and (2) a chain-breaking path leading to carbonyls and alcohols (Figure 1).
- [9] Three depletion mechanisms are known for alkoxy radicals, the reaction with molecular oxygen, thermal

decay, and isomerization (Figure 1) [e.g., Atkinson et al., 1995]. The reaction with O₂, which dominates for small alkoxy radicals, leads to the formation of HO₂ (H-abstraction) and an aldehyde. In the case of the thermal decay generally two smaller organic radicals are formed, which, in turn, rapidly react with atmospheric O₂ to form further peroxy radicals [Atkinson et al., 1995, 1997]. In the case of nitrate oxy radicals it is also possible that separation of NO₂ leads to the formation of stable products breaking the radical chain reaction [e.g., Wängberg et al., 1997]. Isomerization proceeds via H-shift producing an alkyl radical with an OH group. Considering these sinks for alkoxy radicals, under tropospheric conditions the typical lifetimes are less than 1 s.

- [10] Hydro peroxy radicals either react with NO, NO₃, or O₃ to generate hydroxyl radicals or are lost by reactions with other peroxy radials. Taking 40 ppb of ozone, 19 ppt of NO₃, and 9 ppt of NO as an example HO₂ would react with equal rates with the three species. The same destruction rate by self-reaction is gained at 20 ppt HO₂. A further sink of HO₂ (and probably RO₂) is heterogeneous uptake on aerosols [Saylor, 1997].
- [11] Following this reaction scheme of NO₃ with an organic compound (Figure 1) generally a large number of trace species are produced. For α-pinene, which is probably one of the most abundant terpenes in the atmosphere since it is predominately emitted from a number of trees such as Norway Spruce and Scots Pine [e.g., *Janson*, 1993], pinonaldehyde has been identified as the major product. Molar yields have been reported to be close to 0.6 [*Hakola et al.*, 1994; *Wängberg et al.*, 1997].
- [12] In contrast to NO₃-VOC reactions ozonolysis of alkenes can directly produce OH and HO₂ radicals [e.g., *Paulson and Orlando*, 1996; *Ariya et al.*, 2000]. This production is most likely accompanied by the formation of organic peroxy radicals. Ozone adds to the double bond forming a primary ozonoide, which rapidly decompose to form an excited so-called Criegee intermediate and carbonyl products. HO_x radicals are formed in the subsequent decay of the Criegee intermediate. OH yields varying from 7% to 100% were found depending on the structure of the alkene.
- [13] There are several modeling studies predicting nighttime production of peroxy and hydroxyl radicals from NO₃-VOC reactions [Platt et al., 1990; Wayne et al., 1991; Canosa-Mas et al., 1992; Jensen et al., 1992; Le Bras et al., 1993; Mihelcic et al., 1993; Benter et al., 1994; Paulson and Orlando, 1996; Bey et al., 1997, 2001; Carslaw et al., 1997; Gölz et al., 2001], but only few nighttime observations of RO_x radicals can be found in literature [e.g., Cantrell et al., 1997; Clemitshaw et al., 1997; Holland et al., 1998; Grenfell et al., 1999; Kanaya et al., 1999]. Simultaneous measurements of peroxy and nitrate radicals were performed by Mihelcic et al. [1993] and Carslaw et al. [1997]. Mihelcic et al. [1993] presented field measurements of NO₃ and RO₂ radicals at the rural site Schauinsland, Germany, using the matrix isolation electron spin resonance technique (MIESR). Mixing ratios of RO₂ up to 40 ppt were detected and a weak negative correlation of RO₂ and NO₃ was found. The budgets of both radicals could be reproduced by models assuming monoterpene mixing ratios <100 ppt. Mixing ratios of HO_2 and OH up to 10 ppt and 1×10^5 cm⁻³, respectively,

were modeled. Carslaw et al. [1997] found a positive correlation was found between NO_3 and RO_2 in the marine boundary layer near Weyborne, England. An OH production rate of 2×10^4 cm⁻³ s⁻¹ was obtained from a box model.

3. Nighttime Observations of Free Radicals

[14] Simultaneous measurements of NO_3 , O_3 , and RO_x radicals were performed during 15 nights from 20 July to 5 August 1998. The concentrations of NO_3 , O_3 , RO_x , and 50 VOCs were determined continuously during these nights. Intensive studies also including measurements of OH, HO_2 , and RO_2 were done for 20 and 21 July and 4 and 5 August.

3.1. Continuous Measurements

3.1.1. Nitrate Radicals

[15] NO₃ radicals were measured along a light path of 6 km (one way) at a mean height of 18 m using DOAS and in situ at the station by MIESR (height 10 m, 4 and 5 August). Details of the experimental setups used during BERLIOZ are given by *Geyer et al.* [1999]. Measurements of NO₃ were performed during 19 nights. The mixing ratio exceeded the detection limit of 2.4 ppt in 15 nights. Nighttime maxima of NO₃ were usually of the order of 10 ppt; in one night (6 and 7 August) the NO₃ mixing ratio reached 70 ppt [*Geyer et al.*, 2001].

3.1.2. RO_x Radicals

[16] A CA was used to continuously determine the concentration of RO_x from 12 July to 3 August [Volz-Thomas et al., 2003]. During 8 nights (14 and 15 July, 17 and 18 July, 24–26 July, and 3 August) a significant increase of the RO_x mixing ratio after sunset was observed. The average diurnal profile (24 hours) of these days is shown in Figure 2. A daylight maximum of 11.9 \pm 1.1 ppt was found at noon. Then RO_x mixing ratio decreased to 3.6 \pm 0.5 ppt at 1830 UT. While one would expect the decrease to continue (arrow in Figure 2) a second maximum of 6.3 \pm 0.7 ppt appeared between 20 and 22 UT.

3.2. The Night of 20 and 21 July

[17] This night was a typical summer night with temperatures decreasing from 24°C at 20 UT to 15°C at 03 UT and relative humidity rising from 50% at 20 UT to 90% at 03 UT with north wind at very low wind speeds (mean 0.44 m s⁻¹). Sunset and sunrise were, respectively, at 1913 UT and 0315 UT. The chemical regime (Table 1) of this night was determined by very high mixing ratios of organic species [Konrad et al., 2003]. The mixing ratio of α -pinene climbed to 425 ppt, its mean level was 250 ppt (isoprene: maximum 525 ppt, mean 335 ppt). Lumped VOC reactivities with respect to OH, NO₃, and O₃ (defined here as the total reaction frequency of each radical with VOCs, see Table 1) were calculated from the measured concentrations of 27 alkanes, 10 aromatic hydrocarbons, 12 alkenes, isoprene, α-pinene [Konrad et al., 2003], 18 aldehydes [Grossmann et al., 2003] and the modeled concentrations of 8 other monoterpenes [Gever et al., 2001]. In the case of the OH radical the contributions to the VOC reactivity were: isoprene 39%, higher aldehydes 21%, terpenes 7%, and other alkenes 16%. For NO₃

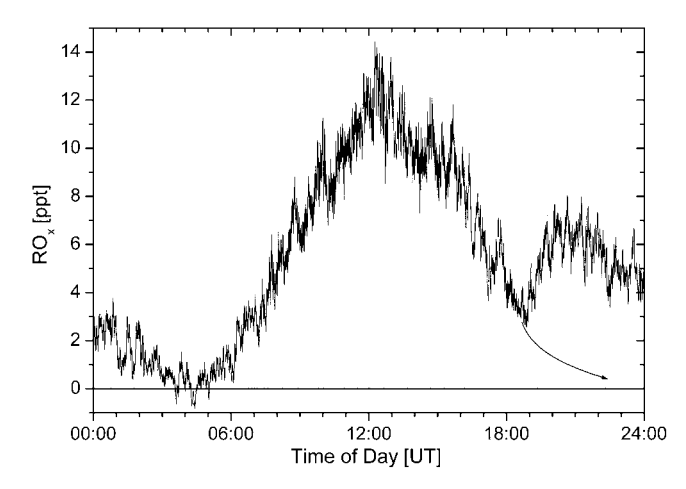


Figure 2. Diurnal profile of the RO_x mixing ratio as measured by the chemical amplifier [*Volz-Thomas et al.*, 2003] averaged for 8 days (14 and 15 July, 17 and 18 July, 24–26 July, and 3 August) with enhanced nighttime production of RO_x at Pabstthum. The arrow at 19 UT illustrates the expected profile without nighttime RO_x production.

monoterpenes were the dominant reaction partner with a contribution of 83% to the VOC reactivity. For ozone the contributions of terpenes, isoprene, and other alkenes were 20%, 20%, and 60%.

[18] Nighttime levels of NO₂ and ozone were both high (NO₂: 5–15 ppb, O₃: 60–10 ppb; Table 1) [Volz-Thomas et al., 2003]. The production rate of NO₃ therefore was high with values of the order of 3 × 10⁶ cm⁻³ s⁻¹. Nevertheless NO₃ remained below its detection limit during this night. This can be attributed to the high degradation frequency of NO₃ arising from reaction with VOCs. The mixing ratio of NO was near or even below the detection limit (20 ppt for a single measurement) during the first part of the night and then continuously rose to 72 ppt at 0203 UT (Table 1). Because of calibration procedures of the in situ monitor at every night between 22 and 23 UT the NO₂ data measured by DOAS [Alicke et al., 2003] was used during this period. The NO mixing ratio was interpolated during this time period.

[19] The mixing ratio of RO_x decreased from 15 ± 5 ppt at 20 UT to 10 ± 5 ppt at 0300 UT. The nighttime levels of OH radicals were measured by laser-induced fluorescence (LIF) starting at 0153 UT [see Holland et al., 2003]. While during other nights the concentration of OH was below the LIF detection limit (the LOD for OH of the LIF is mainly defined by the uncertainty of the ozone interference correction of $(3.2 \pm 0.8) \times 10^5$ OH mol cm $^{-3}$ at 50 ppb ozone) [Holland et al., 2003], the following 20 min averages of the OH concentration were observed in the early morning hours of 21 July: (1.60 \pm 0.85) \times 10⁵ cm⁻³ (0153-0213 UT), (0.71 \pm 0.81) \times 10⁵ cm⁻³ (0213–0233 UT), and (1.85 \pm 0.82) \times 10⁵ cm⁻³ (0233-0253 UT). The errors represent the 2σ error of the mean value during these periods. The mixing ratios of HO_2 during this time period were 4 \pm 0.1, 4.2 \pm 0.2, and 3.9 ± 0.3 ppt.

3.3. The Night 4 and 5 August

[20] 4 and 5 August was a night with clear sky. Temperatures were in the range of 9°-15°C and relative humidity increased from 65% at 20 UT to 95% at 03 UT. Westerly winds with low speeds ($\sim 1 \text{ m s}^{-1}$) were observed. Sunset was at 1850 UT, sunrise at 0338 UT. The ozone level decreased from 27 to 13 ppb. NO₂ was in the range of 2.6– 4.2 ppb (Table 1). The production rate of NO₃ was roughly a factor 3 lower than during the night 20 and 21 July. The mixing ratios of VOCs, in particular of monoterpenes, were low (α-pinene remained below 10 ppt). Lumped VOC reactivities for OH, NO₃, and O₃ (Table 1) were calculated according to section 3.2. Since no aldehyde measurements were performed during this night, a contribution of 20% (value at 20 and 21 July) to the VOC reactivity for OH was assumed for aldehydes. In the case of OH, the following contribution to the VOC reactivity was calculated: alkanes 13%, alkenes 43%, and isoprene 16%. Monoterpenes were the most important organic reaction partner of NO₃ during this night (55% contribution of terpenes to VOC reactivity, 45% from other higher alkenes). The VOC reactivity toward ozone arose mainly (83%) from nonbiogenic alkenes. NO levels increased during the night. At 2027 UT and 0013 UT NO mixing ratio was close to the detection limit. Between 2141 and 2255 UT the NO level was \sim 20 ppt. To the end of the night the NO mixing ratio reached more than 60 ppt (Table 1).

Table 1. Mixing Ratios of Ozone, NO₂, and NO and Total VOC Reactivities Toward Each Radical (Defined Here as the Total Reaction Frequency of Each Radical With VOCs) for the Nights 20 and 21 July and 4 and 5 August 1998 at Pabstthum, Germany, Used as Input Parameters for the Box Models

Date [UT]	O ₃ [ppb]	NO ₂ [ppb]	NO [ppt]	VOC-NO ₃ [10 ⁻² s ⁻¹]	VOC-OH [s ⁻¹]	VOC-O ₃ [10 ⁻⁷ s ⁻¹]
20 July 1998, 1921	57	3.7	5	2.7	2.3	3.8
20 July 1998, 2042	50	3.8	3	5.7	2.5	5.8
20 July 1998, 2203	41	2.9	9	4.5	1.9	5.7
20 July 1998, 2324	39	5.1	19	8.2	2.2	5.8
21 July 1998, 0043	34	5.0	17	10	2.3	6.5
21 July 1998, 0203	28	8.2	72	18	3.1	9.4
04 August 1998, 2027	27	3.7	7	0.55	0.56	0.89
04 August 1998, 2141	24	3.6	20	0.30	0.49	0.85
04 August 1998, 2255	23	3.4	22	0.45	0.50	0.74
05 August 1998, 0013	25	2.6	9	0.37	0.40	0.68
05 August 1998, 0132	17	4.2	63	0.28	0.37	0.64
05 August 1998, 0250	13	4.2	62	0.51	0.44	0.76

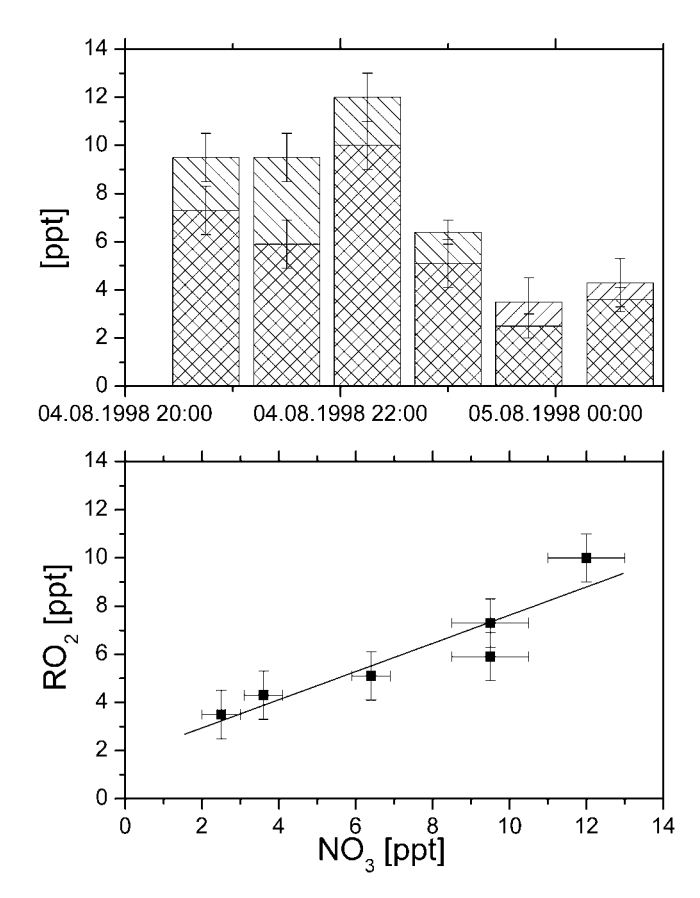


Figure 3. Simultaneous measurements of organic peroxy radicals (checkered) and NO₃(lines) by MIESR [*Mihelcic et al.*, 2003] during the night 4 and 5 August 1998 at Pabstthum. A linear positive correlation between RO₂ and NO₃ was found during this night (slope: 1.8 ± 1.0 , offset: 0.6 ± 0.1 ; R² = 0.86).

[21] From 4 and 5 August simultaneous measurements of nitrate radicals by DOAS and MIESR were performed. The data of both measurement techniques were in good agreement within their uncertainty ranges [Geyer et al., 1999]. After sunset the NO₃ level rapidly increased to 10– 12 ppt from 20 to 22 UT. Then the mixing ratio of nitrate radicals slowly decayed to 2 ppt at 2 UT (Figure 3). The hydroxyl radical level remained below the detection limit of the LIF system. The nocturnal mean of the OH concentration this night as measured by LIF was 0.3 $(+2.3/-0.3) \times 10^5$ cm⁻³. The mixing ratio of HO₂ as determined by LIF continuously decreased from 1.8 ppt at the beginning of the night to 0.5 ppt at 0300 UT. The HO₂ concentration and the sum of organic peroxy radicals (RO₂) were measured by MIESR during this night [see Mihelcic et al., 2003]. The HO₂ radical level was below the detection limit of 1 ppt of the ESR system. The mixing ratio of RO₂ was high at the beginning of the night 4 and 5 August (6 to almost 10 ppt) decreasing in the second half down to <5 ppt (Figure 3).

[22] Comparing the nighttime profiles of NO₃ and RO₂ it is apparent that they are strongly correlated (Figure 3). High peroxy radical mixing ratios were observed at high nitrate radical levels (2215 UT). A linear regression was performed yielding a linear dependence of both species at

a correlation coefficient of R^2 = 0.83: RO_2 = (1.8 ± 1) + (0.59 ± 0.12) · NO_3 .

4. Model Results

4.1. Description of the Box Model

[23] A box model for nighttime radical chemistry was used to model the contributions of NO₃, ozone, and secondary produced OH radicals to nighttime RO_x production. The inorganic section of this model is identical with the updated module of the master chemical mechanism (MCM) [Jenkin et al., 1997, 1999]. It generally consists of the HO_x and NO_x chemistry described above (compare to Table 2). Photochemistry and deposition are not included. The reactions of N₂O₅ and peroxy radicals on aerosol surfaces (Since no aerosol data are available for Pabstthum, the average aerosol surface observed at another site of the campaign (Falkenberg, 14°07′E, 52°10′N) [Wex et al., 2002] was used) are calculated using uptake coefficients of 0.04 and 0.2 [Hu and Abbat, 1997; DeMore et al., 1997]. Lumped reactivities of VOCs with respect to OH, NO₃, and O₃ are used as described in sections 3.2 and 3.3. The reactions of OH, NO₃, or ozone with VOCs directly produce peroxy radicals (RO₂). Although RO₂ is defined as any possible organic peroxy radical that could be produced from VOC oxidation, it will be mostly α pinene-peroxy and isoprene-peroxy (α-pinene and isoprene were the major individual organic reaction partners of OH, NO_3 , and O_3). In the case of ozonolysis a formation yield of OH of 0.7 (yield for α -pinene) [Paulson et al., 1999] was applied. Methyl peroxy radicals are modeled separately. The following rate constants for organic peroxy radical reactions were chosen (Table 2): 5×10^{-12} cm³ s⁻¹ (RO₂ + NO), 3×10^{-12} cm³ s⁻¹ (RO₂ + NO₃), 1×10^{-11} cm³ s⁻¹ (RO₂ + HO₂), and 6×10^{-13} cm³ s⁻¹ (RO₂ + RO₂). Note that at the present time the reaction rates of higher peroxy radicals such as pinene-peroxy are not known. The rates presented here are deduced from the reaction rates of methyl peroxy.

[24] Comparison of the results of this model to that of the master chemical mechanism (which includes the detailed gas-phase tropospheric degradation scheme of 123 VOCs) showed good agreement in the modeled RO_x concentrations (better than 20% for OH and HO₂, better than 40% for RO₂). The uncertainty of the model results arising from the uncertainty of the measured concentrations was obtained by sensitivity studies of the models using the known uncertainty ranges of the input parameters. This study was done for each model run. The model results of RO_x and NO₃ were found to be highly sensitive toward two quantities, the mixing ratios of NO and of monoterpenes (example: Figures 4a-4d, 4 August, 2027 UT). The dependencies of modeled radical mixing ratios on NO and monoterpenes are evident: Taking the sensitivity study of organic peroxy radicals on 4 August, 2027 UT (Figure 4a) as an example, the RO₂ level decreases with increasing NO mixing ratio (because of (1) the fast reaction of RO2 with NO and (2) the decrease of NO₃ via NO₃ + NO resulting in a lower RO₂ production rate). On the other hand, organic peroxy radicals are produced by initial reactions of VOC species, at Pabstthum mainly from monoterpenes [Geyer et al., 2001], with

Table 2. Reactions and Rate Coefficients Used in the Box Model

```
Reaction
                                                                                                                                                                                                           Rate constant [cm<sup>3</sup> s<sup>-1</sup>]
                                                                                                                                                                                                       \begin{array}{l} 2\times 10^{-12}\exp(-1400/T)^{a} \\ 1.2\times 10^{-13}\exp(-2450/T)^{a} \end{array}
NO + O_3 \rightarrow NO_2
NO_2 + O_3 \rightarrow NO_3 + O_2
                                                                                                                                                                                    k_{rec}^{~a} \left\{ \begin{array}{l} k_o = 2.2 \times 10^{-30} (T/300)^{-3.9} cm^6 s^{-1} \\ k_\infty = 1.5 \times 10^{-12} (T/300)^{-0.7}. \end{array} \right.
NO_2 + NO_3 \rightarrow N_2O_5
                                                                                                                                                                                                    k_{rec}/2.7 \times 10^{-27} \exp(11000/T)^a

4.5 \times 10^{-14} \exp(-1260/T)^a
N_2O_5 \rightarrow NO_2 + NO_3
NO_3 + NO_2 \rightarrow NO + NO_2
                                                                                                                                                                                                       8.5 \times 10^{-13} \exp(-2450/T)^{a}
1^{b}
NO_3 + NO_3 \rightarrow NO_2 + NO_2
NO_3 + VOCNO_3 \rightarrow RO_2
                                                                                                                                                                                                           1.5 \times 10^{-11} \exp(170/T)^{a}
2.6 \times 10^{-22c}
NO_3 + NO \rightarrow NO_2 + NO_2
N_2O_5 + H_2O \rightarrow HNO_3 + HNO_3
                                                                                                                                                                                                                     1.9 \times 10^{-39c}
N_2O_5 + H_2O + H_2O \rightarrow HNO_3 + HNO_3 + H_2O
                                                                                                                                                                                                                       \gamma = 0.04^{d}
N<sub>2</sub>O<sub>5</sub> + aerosols -
CH_3O_2 + NO_2 \rightarrow CH_3O_2NO_2
                                                                                                                                                                                     k_{rec}^{~~a} \left\{ \begin{array}{l} k_o = 1.5 \times 10^{-30} (T/300)^{-4} cm^6 s^{-1} \\ k_\infty = 6.5 \times 10^{-12} (T/300)^{-2} \end{array} \right.
                                                                                                                                                                                                    k_{rec}/1.3 \times 10^{-28} \exp(11200/T)^a
1.2 \times 10^{-12a}
3.8 \times 10^{-12} \exp(-800/T)^a
1 \times 10^{-13} \exp(-190/T)^a
CH_3O_2NO_2 \rightarrow CH_3O_2 + NO_2
CH_3O_2 + NO_3 \rightarrow HO_2 + CH_2O + NO_2

CH_3O_2 + HO_2 \rightarrow CH_3OOH
\text{CH}_3\text{O}_2 + \text{CH}_3\text{O}_2 \rightarrow \text{HO}_2 + \text{HO}_2 + \text{CH}_2\text{O} + \text{CH}_2\text{O}
                                                                                                                                                                                                        1.5 \times 10^{-13} \exp(-190/T)^{a}
3 \times 10^{-12} \exp(-280/T)^{a}
CH_3O_2 + CH_3O_2 \rightarrow CH_2O + CH_3OH
CH_3O_2 + NO \rightarrow HO_2 + CH_2O + NO
                                                                                                                                                                   2.3 \times 10^{-13} \exp(600/T) \times (1+1.4 \times 10^{-21} \times H_2O \exp(2200/T))^a
HO_2^{-} + HO_2 \rightarrow H_2O_2
                                                                                                                                                                                    k_{rec}^{~a} \left\{ \begin{array}{l} k_o = 1.8 \times 10^{-31} (T/300)^{-3.2} cm^6 s^{-1} \\ k_\infty = 4.7 \times 10^{-12} (T/300)^{-1.4} \end{array} \right.
HO_2 + NO_2 \rightarrow HO_2NO_2
                                                                                                                                                                                                   k_{rec}/2.1 \times 10^{-27} \exp(10900/T)^a
3.5 \times 10^{-12a}
1.1 \times 10^{-14} \exp(-500/T)^a
3.5 \times 10^{-12} \exp(250/T)^a
\gamma = 0.2^d
HO_2NO_2 \rightarrow HO_2 + NO_2
HO_2 + NO_3 \rightarrow OH + NO_2
HO_2 + O_3 \rightarrow OH
HO_2 + NO \rightarrow OH + NO_2
HO_2 + aerosols \rightarrow
                                                                                                                                                                                                                     2.2\times10^{-11a}
OH + NO_3 \rightarrow HO_2 + NO_2
                                                                                                                                                                                    k_{rec}^{~a} \left\{ \begin{array}{l} k_o = 2.5 \times 10^{-30} (T/300)^{-4.4} cm^6 s^{-1} \\ k_\infty = 1.6 \times 10^{-11} (T/300)^{-1.7} \end{array} \right.
OH + NO_2 \rightarrow HNO_3
                                                                                                                                                                                                   1.3 × 10<sup>-12</sup> exp(380/T)<sup>a</sup>

1.5 × 10<sup>-13</sup> × (1+ 0.6 p(atm))<sup>a</sup>

7.7 × 10<sup>-12</sup> exp(-2100/T)<sup>a</sup>

2.90 × 10<sup>-12</sup> exp(-160/T)<sup>a</sup>

1.6 × 10<sup>-12</sup> exp(-940/T)<sup>a</sup>

2.45 × 10<sup>-12</sup> exp(-1775/T)<sup>a</sup>
OH + HO_2NO_2 \rightarrow NO_2
OH + CO \rightarrow HO_2
OH + H_2 \rightarrow HO_2
OH + H_2O_2 \rightarrow HO_2
OH + O_3 \rightarrow HO_2
OH + CH_4 \rightarrow CH_3O_2
                                                                                                                                                                                                         4.8 \times 10^{-11} \exp(250/T)^a
OH + HO_2 \rightarrow
OH + VOCOH \rightarrow RO_2
                                                                                                                                                                                                        4.2\,\times\,10^{-12}\,\exp(-240/T)^a
OH + OH -
                                                                                                                                                                                    k_{rec}^{\phantom{rec}a} \bigg\{ \begin{array}{l} k_o = 7.4 \times 10^{-31} (T/300)^{-2.4} cm^6 s^{-1} \\ \nu & 3.2 \cdots \end{array} \label{eq:krec}
OH + NO \rightarrow HONO
                                                                                                                                                                                                                    k_{\infty} = 3.2 \times 10^{-11}
                                                                                                                                                                                                       1.80 \times 10^{-11} \exp(-390/T)^{a} \\ 3 \times 10^{-12e}
OH + HONO \rightarrow NO_2
RO_2 + NO_3 \rightarrow HO_2 + RCOR + RCOR
                                                                                                                                                                                                                       1 \times 10^{-11e}
RO_2 + HO_2 \rightarrow ROOH
RO_2 + RO_2 \rightarrow HO_2 + HO_2 + RCOR + RCOR

RO_2 + RO_2 \rightarrow RCOR + ROH
                                                                                                                                                                                                                       2\,\times\,10^{-13e}
                                                                                                                                                                                                                       4\,\times\,10^{-13e}
                                                                                                                                                                                                                       2 \times 10^{-13e}
RO_2 + CH_3O_2 \rightarrow HO_2 + HO_2 + RCOR + CH_2O
                                                                                                                                                                                                                       4 \times 10^{-13e}
RO_2 + CH_3O_2 \rightarrow ROH + CH_2O
                                                                                                                                                                                                                       5 \times 10^{-12e}
RO_2 + NO \rightarrow HO_2 + RCOR + NO_2
                                                                                                                                                                                                                          \gamma = 0.2^d
RO_2 + aerosols \rightarrow
                                                                                                                                                                                                                             0.7^{b/f}
O_3 + VOCO_3 \rightarrow OH + RO_2
```

free radicals. As a consequence the model predicts a positive linear relation between RO₂ and the terpene mixing ratio was modeled. Both mixing ratios, that of NO and of terpenes were low and near their detection

limits at this time. The relative uncertainty interval of the mixing ratio of NO at 2027 UT was 0-17 ppt [Volz-Thomas et al., 2003]. The mixing ratio of terpenes is uncertain within 10-24 ppt [Konrad et al., 2003]. The

^aDe More et al. [1997].

^bFor the reactions of NO₃, OH, and O₃ with VOCs, the corresponding rate coefficients [Atkinson, 1997; Martinez et al., 1999] have been weighted according to the observed concentrations of 50 VOCs.

^cMentel et al. [1996].

^dUptake coefficient of N_2O_5 is given by *Hu and Abbatt* [1997] and $\gamma(HO_2)$ by *Gershenzon et al.* [1995]; $\gamma(RO_2)$ set to value of $\gamma(HO_2)$.

^eSee text.

^fYield for α-pinene [Paulson et al., 1999].

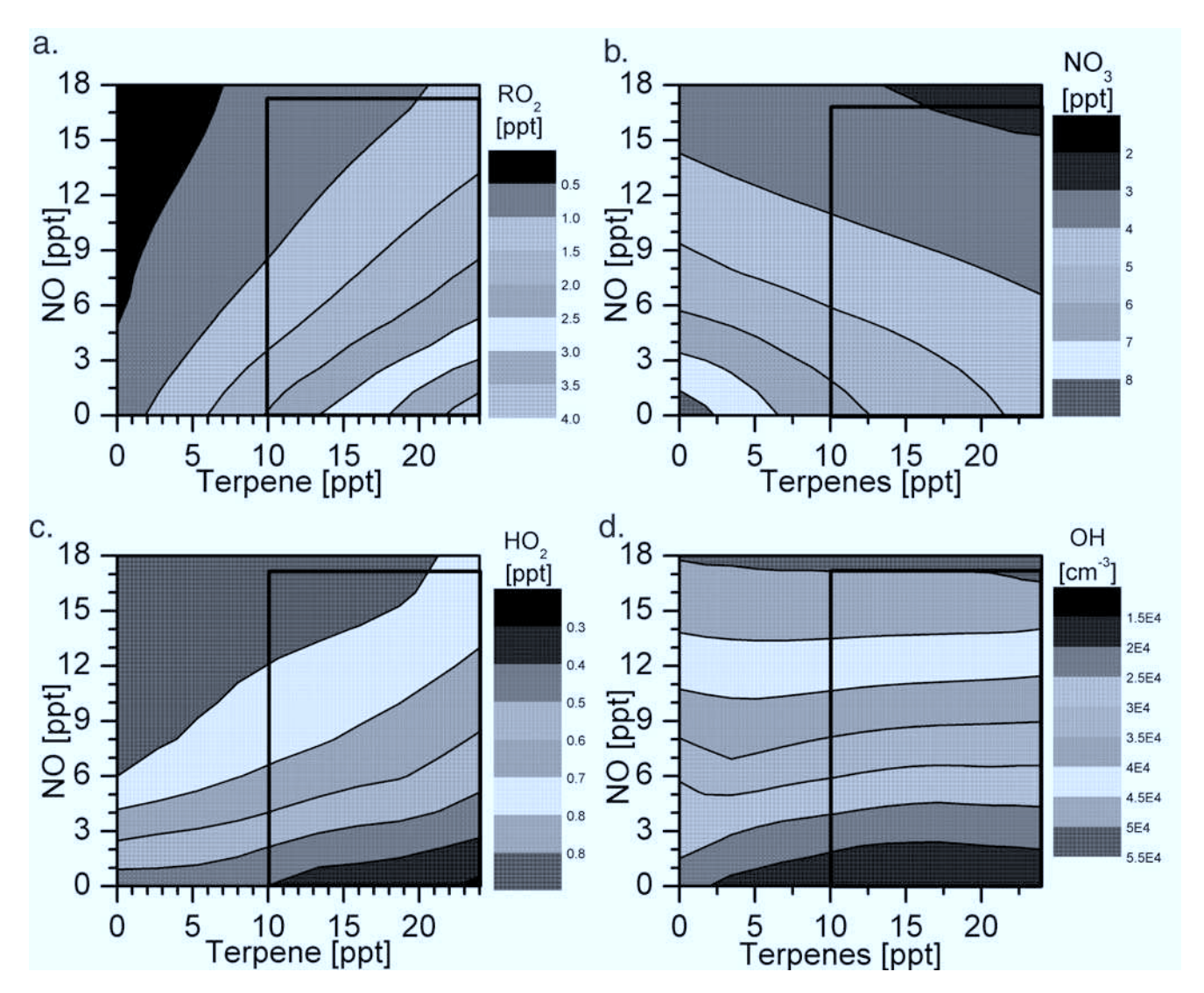


Figure 4. Sensitivity study of the modeled mixing ratios of RO₂ (a), NO₃ (b), and HO₂ (c) and the concentration of OH (d) on the mixing ratios of NO and monoterpenes for 4 August 1998, 2027 UT at Pabstthum, Germany. See color version of this figure at back of this issue.

box in Figure 4 shows the propagation of the uncertainties of the input data onto the modeled RO_2 mixing ratio (23 \pm 17 ppt). Since from 4 and 5 August both, the NO and the terpene mixing ratios were very low, the uncertainty of the model results is high. During most other nights (e.g., 20 and 21 July) the uncertainties of the RO_x mixing ratios are considerably smaller.

4.2. Model Results of the Night 20 and 21 July

[25] The model results of the night 20 and 21 July are presented in Figure 5. Modeling runs were performed during the sampling time of the gas chromatograph [Konrad et al., 2003]. Other input parameters were averaged or interpolated for this time period. The modeled concentrations of the nitrate radical are all below the detection limit of the DOAS system as it was the case for the measurements. The low NO₃ concentration results from the high terpene and NO levels (22–2 UT) during this night. The modeled mixing ratio of NO₃ (Figure 5a) continuously decreased from 2.2 ppt at 2042 UT to 0.5 ppt in the early

morning. Steady state mixing ratios of N₂O₅ are modeled in the range of 5.5 ppt to 8.8 ppt. Modeled OH levels (Figure 5b) were $(1.5-2) \times 10^5$ cm⁻³ during most of the night jumping to $(4.1 \pm 0.7) \times 10^5$ cm⁻³ at 0203 UT (approximately 1 hour before sunrise). The model shows that most of the OH was produced by ozonolysis during this night. The mean contribution to OH production by nitrate radicals was 26% during this night. The high nighttime concentration of OH at 2 UT corresponds to 20% of a typical daytime level of 2×10^6 cm⁻³ [Hein et al., 1997] and to 7% of the OH measurements at 20 and 21 July from 10 to 11 UT of 6×10^6 cm⁻³ at Pabstthum [Holland et al., 2003]. Comparing the model results at 0203 UT with the concentration of $(1.6 \pm 0.85) \times 10^5$ cm⁻³ measured by the LIF system at the same time (Figure 5b), the model is overestimating the OH concentration. This could point to an underestimation of OH sinks by the model as also found by daytime model studies [Mihelcic et al., 2003]. More nighttime measurements of OH, however, are needed to strengthen this hypothesis.

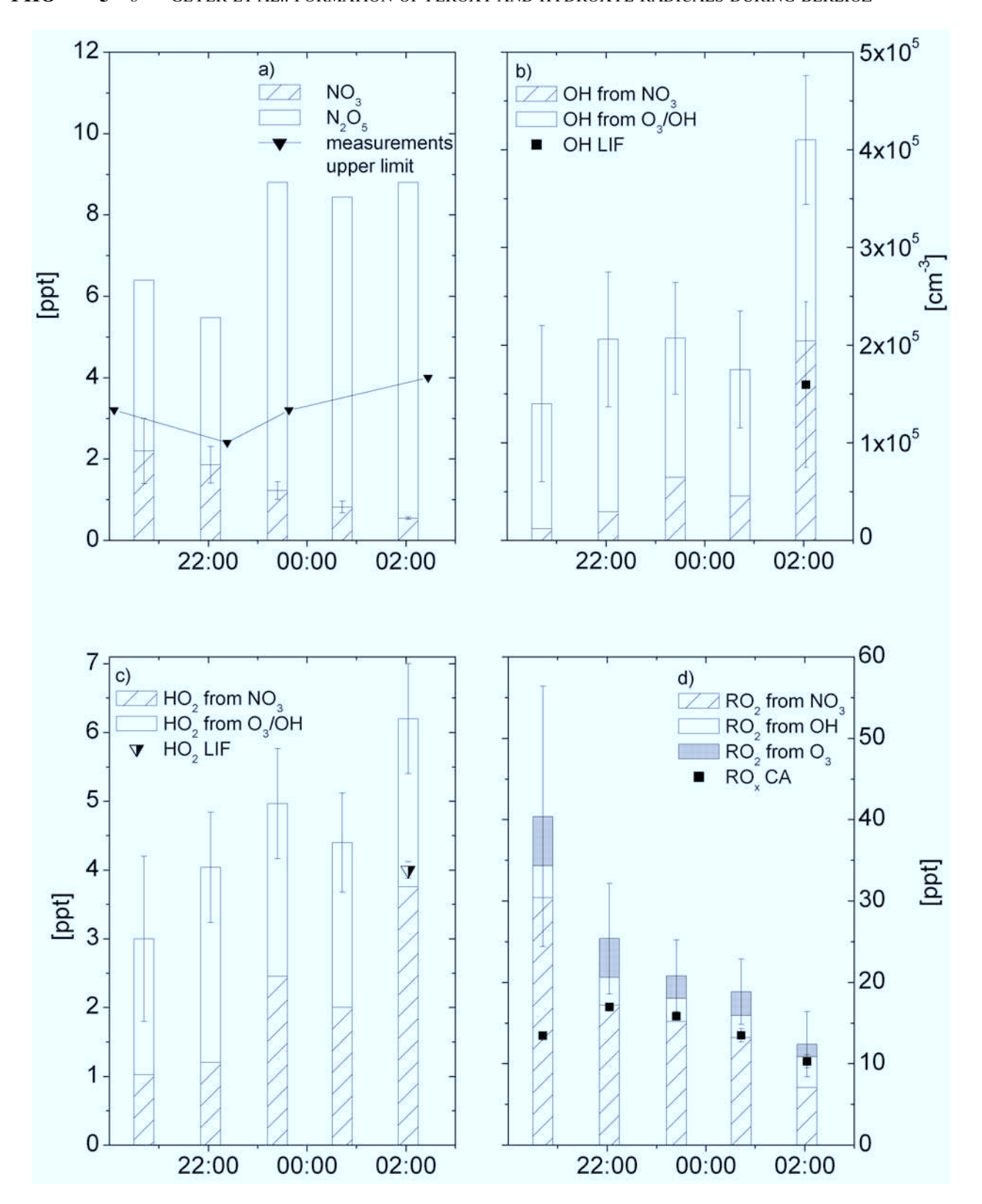


Figure 5. Model results of NO_3 and N_2O_5 (a), OH (b), HO_2 (c), and RO_2 (d) for the night 20 and 21 July 1998 at Pabstthum. The modeled mixing ratios of the RO_x radicals are separated regarding their production path by NO_3 , O_3 , and OH (in the case of RO_2) reactions with VOCs. Also included are the observed levels of OH and HO_2 at 0203 UT (LIF) and of RO_x (CA). The modeled levels of NO_3 remain below the upper limits of the measurements. At 0203 UT, an OH concentration of $(4.1 \pm 0.7) \times 10^5$ cm⁻³ was modeled, which is significant higher than the measured value of $(1.6 \pm 0.85) \times 10^5$ cm⁻³ at this time. While organic peroxy radicals were produced mainly by NO_3 -VOC reactions, ozonolysis was the major source of OH and HO_2 during this night.

The mixing ratios of $\rm HO_2$ radicals predicted by the model (Figure 5c) are increasing during the night. At 0203 UT a $\rm HO_2$ level of 5.6 \pm 0.4 ppt is modeled. This is slightly higher than the ambient observation of $\rm 4 \pm 1$ ppt by LIF (Figure 5c). The mean contribution of $\rm NO_3$ to the production of $\rm HO_2$ radicals was 44% during this night. The calculated mixing ratio of the sum of organic peroxy radicals (Figure 5d) decreased from 40 ppt at 2042 UT to 14 ppt at 0203 UT. The modeled levels of $\rm RO_2$ are slightly higher than the values observed by the CA (decreasing from 18 ppt at 22 UT to 10 ppt at 2 UT, see Figure 5d). It was found that most of the organic peroxy radicals were produced by the reaction of $\rm NO_3$ with VOCs (70%). The contribution of OH + VOCs and ozonolysis to the $\rm RO_2$ production was 15% each.

4.3. Model Results of the Night 4 and 5 August

[26] For this night model runs were performed (1) using the measured NO₃ values as input parameters and (2) with NO₃ resulting from the model. In case 1 the NO₃ data from the MIESR system (which were in good agreement with the NO₃ data from the DOAS system) [Geyer et al., 1999] were used since these were measured in situ at the station at Pabstthum.

[27] Case 1: The model results together with the NO₃ input mixing ratios (10-12 ppt in the first half of the night) are shown in Figure 6. A maximum concentration of OH of $(1.4 \pm 0.4) \times 10^5$ cm⁻³ was modeled at 2255 UT (Figure 6b), which is below the detection limit of the LIF system. The modeled HO₂ level was high (as was the OH level) until about midnight with mixing ratios of 2.8-4 ppt (Figure 6c). Then OH and HO₂ decreased continuously until sunrise (probably because NO3 decreased (less production of HO₂) while NO increased (higher destruction of HO₂)). The trend and order of magnitude of the modeled HO₂ concentration are comparable to the observations of HO₂ by LIF (Figure 6c) [Holland et al., 2003]. The modeled mixing ratios of organic peroxy radicals are higher than the ambient observations of the MIESR system (Figure 6d). Nevertheless, within the error of the modeled concentrations, which is largely due to the strong dependence of RO₂ on NO and terpenes, both data sets are in agreement. The contribution of NO₃ to the production of the RO_x radicals was considerably higher compared to the night 20 and 21 July. Contributions of 78%, 88%, and 92% were found for OH, HO2, and RO2, respectively. These high contributions demonstrate the potential importance of nitrate radicals for the nighttime production of RO_x.

[28] Case 2: To the beginning of the night the modeled NO_3 mixing ratio ranged from 2 to 4.4 ppt. Then the NO_3 level decreased to values below 1 ppt at 0132 UT and 0250 UT. The steady state mixing ratio of N_2O_5 was in the range of 10 ppt to 34 ppt. Compared to ambient observations the modeled NO_3 mixing ratios are a factor 2–3 too low. This trend was also observed during other nights and could indicate that the N_2O_5 sink on aerosols is overrated by the model (note that the aerosol data is from another site of the campaign). It could also be attributed to the high sensitivity of the modeled NO_3 toward the NO mixing ratio (section 4.1). Calculations by *Geyer et al.* [2001] showed that the NO mixing ratio is much lower along the DOAS light path (mean height: 18 m) than at the

height of the NO measurements of 10 m because the source of NO is probably the soil.

4.4. Summarized Model Results of BERLIOZ

[29] The concentrations of NO₃, OH, HO₂, and RO₂ are modeled for all nights during the BERLIOZ campaign (20 July to 6 August) when VOC data is available. The mean modeled mixing ratio of NO₃ is 2.2 ppt. The following mean nighttime levels of RO_x radicals are modeled during BERLIOZ: OH concentration: $(6 \pm 1) \times 10^4$ cm⁻³ (average if excluding the night 20 and 21 July: $(4 \pm 1) \times 10^4$ cm⁻³), HO₂ mixing ratio: 1.0 ± 0.2 ppt, RO₂ mixing ratio: 5.2 ± 0.3 ppt.

[30] The mean measured nighttime levels are: For OH radicals, an upper limit of $(4 \pm 1) \times 10^4$ mol cm⁻³ was determined by *Holland et al.* [2003] excepting the night 20 and 21 July. The mean modeled OH concentration is just in within the upper limit of the LIF measurements. The average mixing ratio and the variability of HO_2 in the time window from 2100 UT to 0300 UT were 1.2 ppt and 0.5 ppt, respectively [*Holland et al.*, 2003]. The model results are in good agreement with these values. For RO_2 the CA measured an average mixing ratio of 4 ppt [*Volz-Thomas et al.*, 2003], which is in good agreement with the modeled levels.

[31] The mean modeled ratio of nighttime RO₂/HO₂ was 6.5 varying from 0.4 to almost 36. The contribution of NO₃ radicals to the production of OH, HO₂, and RO₂ was calculated by comparing model runs using the measured NO₃ concentrations to runs with the NO₃ concentration fixed to zero. The same comparison was performed for O₃ (measured data) and OH (modeled values). During the campaign nitrate radicals are found responsible for 36%, 53%, and 77% of the nighttime OH, HO₂, and RO₂ production, respectively. Nighttime ozonolysis produced 12% of the RO₂ radicals but 64% of the OH radicals (47% of the HO₂ radicals). The modeled mean contribution of nighttime OH radicals to the organic peroxy radical production was 11%.

[32] During 4 nights (24-26 July) and 3 August) with enhanced nighttime RO_x production measurements (by the CA) and model studies are overlapping. Figure 7 shows the average diurnal profile (on a hourly basis) of the RO_x concentrations for these nights for both, model results and observations. Both data series show a broad peak around 20 UT. The model is slightly underestimating the ambient concentrations.

5. Discussion

5.1. Correlation of NO₃ and RO₂

[33] On a first view the correlation between NO₃ and RO₂ is not clear. On the one side RO₂ is produced partly by the reaction of NO₃ with VOCs, which suppose a positive correlation of both concentrations. On the other side RO₂ can react with NO₃ (Figure 1) what could lead to a negative correlation. The measured data strongly suggests a positive correlation (Figures 3 and 7). A clear positive correlation in every night was also found by the model. The slope of RO₂ versus NO₃, however, is different from night to night. The following discussion is restricted to the nights 20 and 21 July (squares in Figure 8) and 4 and 5 August (triangles in

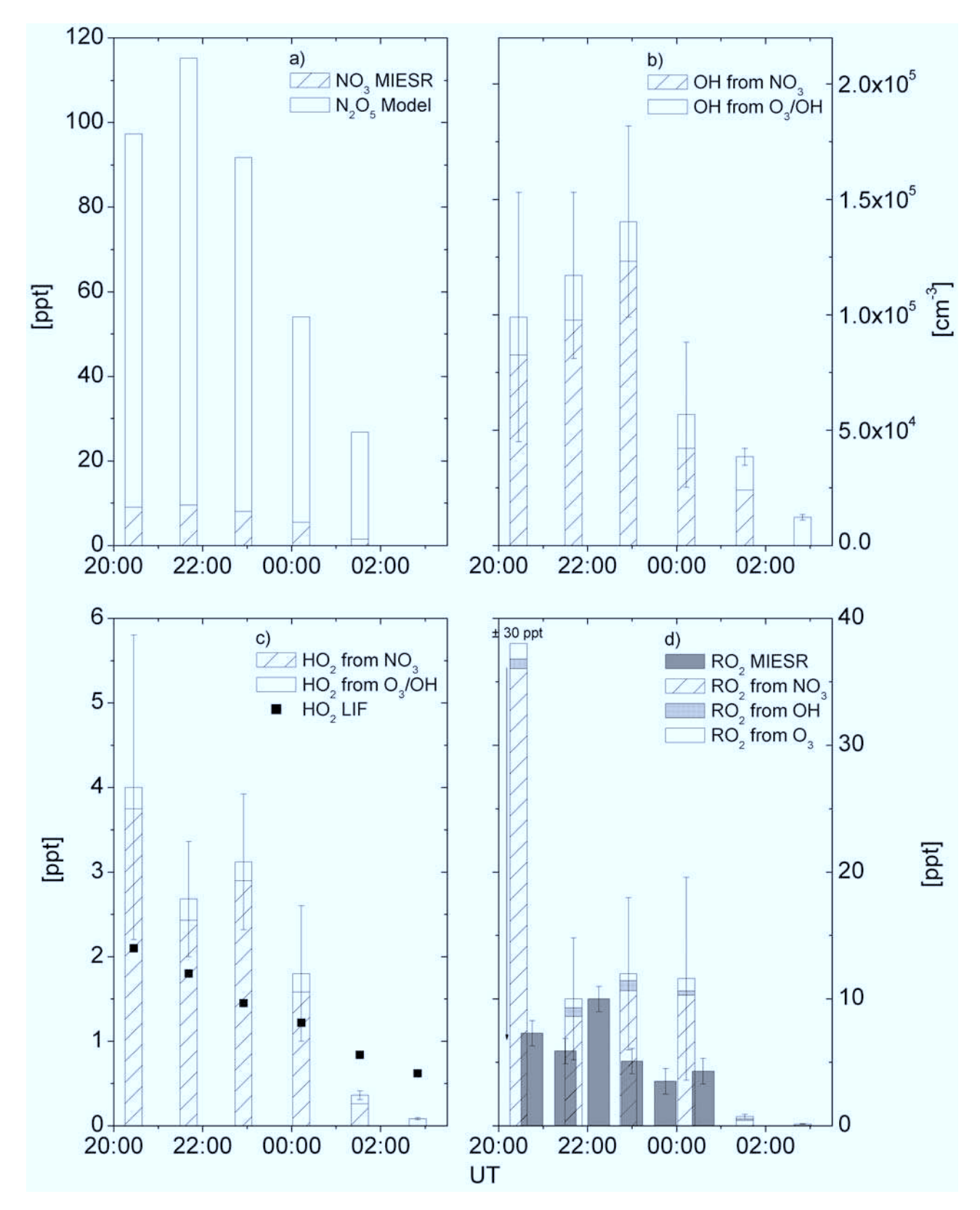


Figure 6. Model results of N_2O_5 (a), OH (b), HO_2 (c), and RO_2 (d) for the night 4 and 5 August 1998 at Pabstthum using the NO_3 data observed by MIESR (a) as input parameter. The mixing ratios of the RO_x radicals are separated regarding their production path by NO_3 , O_3 , and OH (in the case of RO_2) reactions with VOCs. Also included are the HO_2 and RO_2 mixing ratios observed at the site (by MIESR). The OH concentration remained below the detection limit during this night.

Versus RO₂

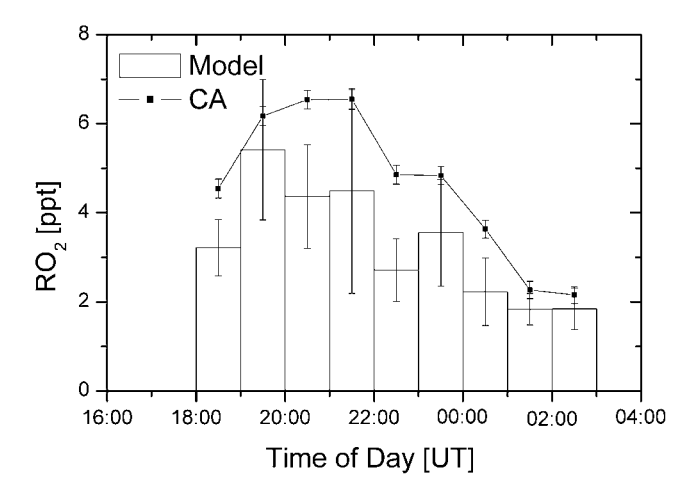


Figure 7. Comparison of the modeled and observed (CA) [Volz-Thomas et al., 2003] nighttime profile of the RO_x mixing ratio averaged for 24–26 July and 3 August 1998 at Pabstthum. The error bars refer to 2σ uncertainty.

Figure 8). The chemical behavior during all other nights was similar to that of 4 and 5 August. A comparison of both nights (see also Table 1) shows that during the night 20 and 21 July:

- 1. The NO₃ production rate was roughly a factor 3 higher.
- 2. The NO_3 degradation frequency from the $NO_3 + NO$ reaction was 50% lower.
- 3. The NO₃ degradation frequency from NO₃ + VOC reactions was a factor 20 higher.

5.1.1. Discussion of 20 and 21 July

[34] Because of the very high VOC reactivity during the night 20 and 21 July NO₃ + VOC reactions were the only important loss path of NO₃ leading to a negative correlation of the NO₃ mixing ratio and the VOC reactivity (Figure 9a). Since the RO₂ production rate is calculated from the product of NO₃ and VOC reactivity (note that both quantities are negatively correlated) no dependence was found between the NO₃ mixing ratio and the RO₂ production rate (Figure 9b). The positive correlation of peroxy and nitrate radicals can therefore not be explained by the production reaction of RO₂ by NO₃. In our opinion the positive correlation of RO₂ and NO₃ appeared because of the dependence of both mixing ratios toward ambient NO levels: As already stated above reactions of NO₃ with NO were of less importance during this night and cannot explain the negative correlation of NO₃ and NO found by the model (Figure 9c). This can properly be attributed to a positive correlation between NO and the VOC reactivity observed during this night (possibly because of the dependence of both mixing ratios on the mixing layer height or coupled biogenic emissions of NO). Because reactions of RO2 with NO were the most important sink of RO2 during 20 and 21 July, the mixing ratios of RO2 and NO were also negatively correlated (Figure 9d).

5.1.2. Discussion of 4 and 5 August

[35] As a consequence of the high NO and low VOC levels during the night 4 and 5 August NO₃ + VOC reactions were of almost no importance as NO3 sink. Therefore no correlation between NO₃ and the VOC reactivity was found (Figure 9e, note that the data in Figure 9

refers to the case 2 of section 4.3, i.e., NO₃ values were modeled not measured). Because most of the RO2 radicals were produced by NO₃ + VOC reactions (section 4.3) a clear positive correlation between the NO₃ mixing ratio and the RO₂ production rate could be modeled (Figure 9f). In addition a negative correlation between NO₃ and NO was found because NO₃ + NO reactions were the most important NO₃ sink (Figure 9g). With the same argument as in section 5.1.1 the RO₂ mixing ratio is also negatively correlated to NO (Figure 9h). The positive correlation of RO₂ and NO₃ during 4 and 5 August originated therefore from the dependence of both radicals on NO and the production of RO₂ by VOC-NO₃ reactions.

[36] The modeled linear factor between RO₂ and NO₃ of 1.8 ± 0.3 in the night 4 and 5 August can be compared to the factor 0.6 ± 0.1 observed by MIESR (Figure 3). The difference between the two factors arises from the underestimation of NO₃ by the model as discussed in section 4.3. 5.1.3. Comparison With Previous Observations of NO₃

[37] The results of this paper have to be compared to previous simultaneous observations of NO₃ and RO₂ in the boundary layer. While Carslaw et al. [1997] also found a positive correlation of RO2 and NO3 at the Weyborne Atmospheric Observatory on the eastern coast of England, Mihelcic et al. [1993] detected a weak negative correlation of RO₂ and NO₃ at the rural site Schauinsland, Germany. There are three important prerequisites of a negative correlation of RO₂ and NO₃: VOCs have to be the dominant sink of NO₃; nighttime NO has to be negligible as a NO₃ sink; and the NO₃ production rate has to be independent from the VOC level. Under these conditions, which are typical for rural forested areas (like Schauinsland) model runs result in a negative correlation of NO₃ and RO₂ originating from chances of the VOC reactivity. At increasing VOC reactivity nitrate radicals are removed faster resulting in a lower steady state concentration of NO₃. On the other side the production rate of RO₂ increases at higher VOC reactivity

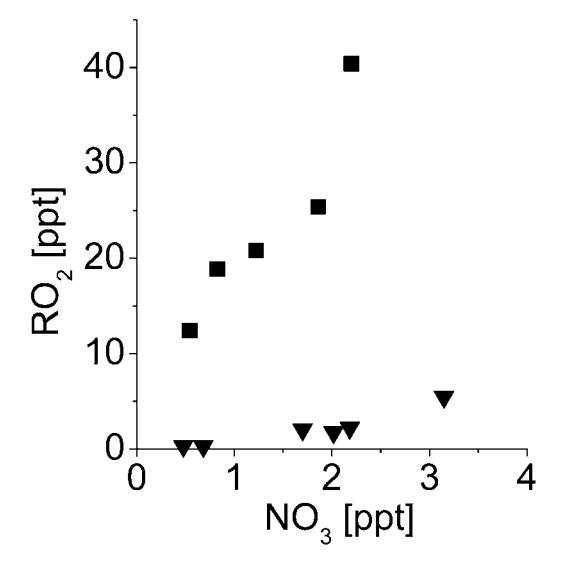


Figure 8. Positive correlation of the modeled mixing ratios of RO₂ and NO₃ for the nights 20 and 21 July (squares) and 4 and 5 August (triangles).

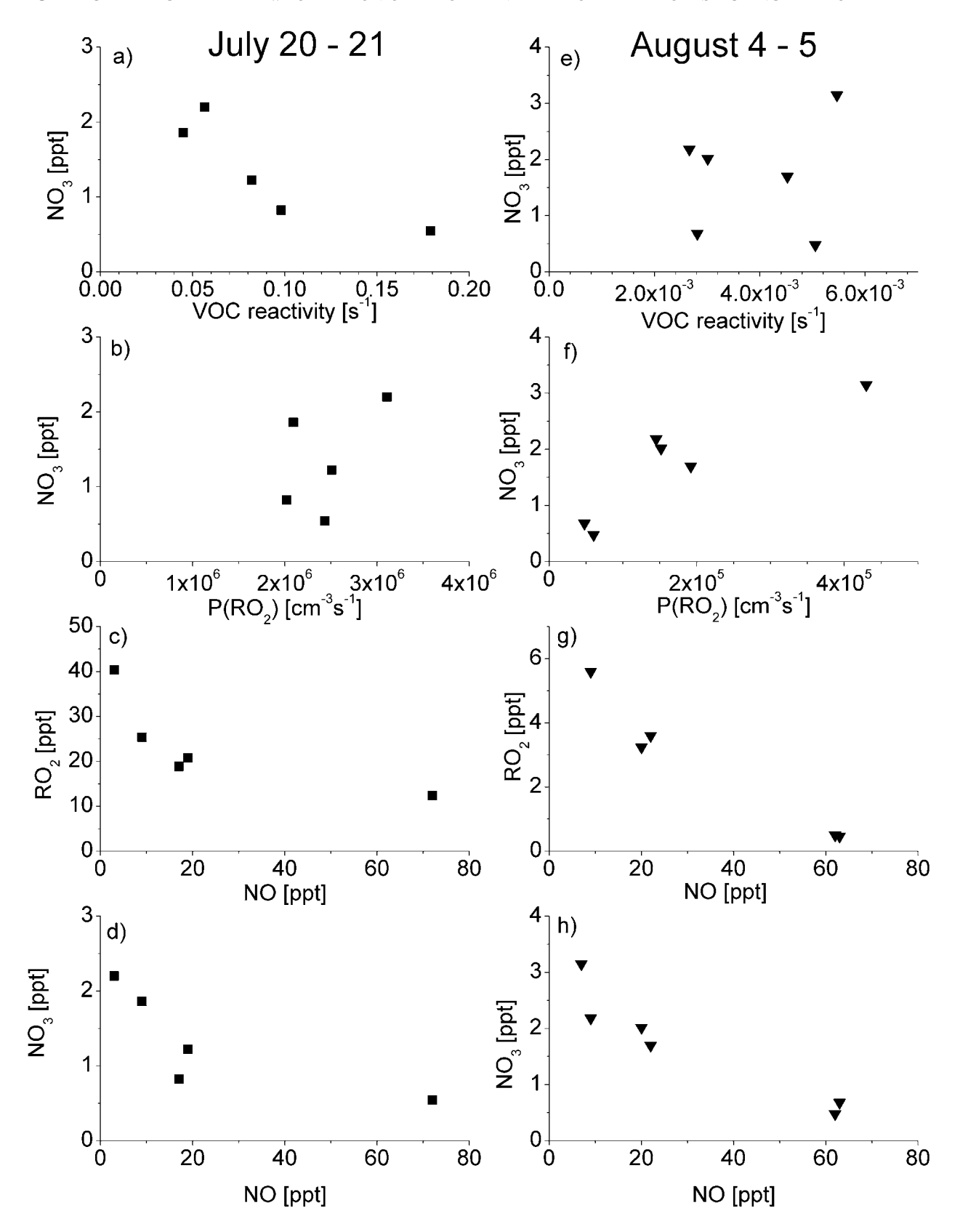


Figure 9. Correlation studies of the origin of the modeled positive dependence of peroxy radicals on the mixing ratios of NO₃ at Pabstthum. The left column refers to 20 and 21 July (squares), the column to the right to 4 and 5 August (triangles, case 2 in section 4.3). (a) and (e) NO₃ (model) versus measured VOC reactivity, (b) and (f) NO₃ (model) versus production rate of RO₂ (calculated from measured VOC reactivity and modeled NO₃), (c) and (g) RO₂ (model) versus NO (measurements), and (d) and (h) NO₃ (model) versus NO (measurements).

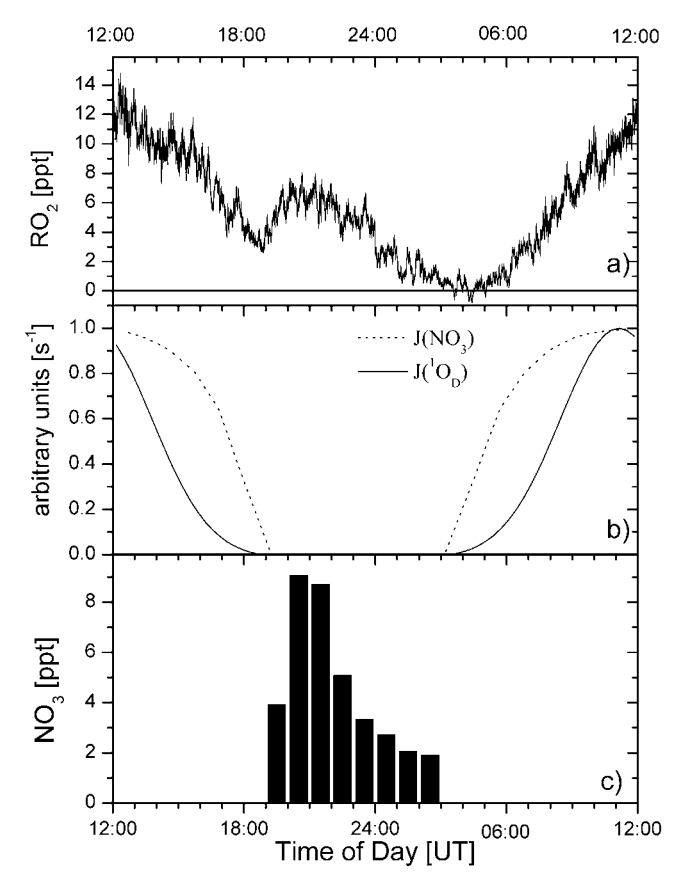


Figure 10. The measured diurnal profile of the RO_x mixing ratio for 8 days (14 and 15 July, 17 and 18 July, 24– 26 July, and 3 August) at Pabstthum from Figure 2a in relation to the photolysis frequencies of NO₃ and ¹O_D (Figure 2b) (filter radiometers) and the variation of the NO₃ mixing ratio (DOAS measurements) during these nights (Figure 2c).

(e.g., by ozonolysis) and the RO2 degradation frequency decreases (by reactions of NO₃ and RO₂) leading to a net raise of the RO₂ concentration.

5.2. Diurnal Profile of RO_x

[38] During daytime the measured mean profile of RO_x shown in Figure 10 can be understood in terms of photochemical production as discussed by Volz-Thomas et al. [2003]. In Figure 10 this profile (a) was related to the mean modeled photolysis frequencies of ozone J(1OD) and of J(NO₃) of these days (b). Both frequencies were normalized to 100% to compare their relative shape. Since NO₃ is photolyzed in the red spectral region, J(NO₃) is already/still high in the early morning and late afternoon, when $J(^{1}O_{D})$ is still/already very low. Between 17 UT and 19 UT, the concentrations of both radicals, hydroxyl radicals which are mainly produced by the photolysis of ozone [Alicke et al., 2003] and nitrate radicals, which are photolyzed rapidly, are very low leading to the minimum of RO_x concentration observed during this time period. The trend of the RO2 concentration (rapid increase at 19 UT, high level between 19 UT and 22 UT, then continuous decrease until 5 UT) is justified by the positive correlation of RO₂ and NO₃ discussed in section 5.1 and the mean diurnal profile of NO₃ shown in Figure 10c. A dependence of RO_x on the VOC reactivity is not visible: The VOC reactivities toward OH and NO₃ have a maximum around 6 UT (probably because of the low mixing layer at this time), when the RO_x level reached a minimum.

5.3. Correlation of NO₃ and OH

[39] The correlation of OH and NO₃ for the nights 20 and 21 July and 4 and 5 August is shown in Figure 11. During 20 and 21 July a negative correlation was found: OH levels increased while the NO₃ concentration decreased. During this night OH was produced mainly by ozonolysis: the contribution of ozonolysis to OH production was 75% (section 4.2). The origin of the negative correlation is the strong coupling of both radicals to VOC reactivity. As already stated above most of the OH was produced by ozonolysis during this night (the ozone mixing ratios were about two times higher from 20 and 21 July) resulting in a correlation of OH concentration and the VOC reactivity of ozone. The VOC reactivity of ozone is well correlated with that of NO₃ since both react only with unsaturated VOCs. The concentration of NO₃ was negatively correlated with the reactivity of VOCs for NO₃. Contrary during 4 and 5 August, no dependence was modeled (Figures 9a/9e). This change of the correlation's slope can be attributed to the high contribution of nitrate radicals to the OH production of 78% (section 4.3) during this night.

5.4. Increase of Oxidation Capacity by Nighttime OH

[40] The enhanced nighttime levels of OH can influence the nighttime oxidation capacity of the atmosphere. The oxidation capacity is defined as the degradation rate [unit: cm⁻³ s⁻¹] of VOCs, CO, and methane due to the attack of free radicals. It is calculated according to Geyer et al. [2001] using the VOC reactivities toward OH and, in a first step, the modeled OH concentrations. Also included is the oxidation of CO (measured) and CH₄ (set to 1.8 ppm) by OH. Nighttime oxidation capacities of OH between 0.1×10^5 and 17×10^5

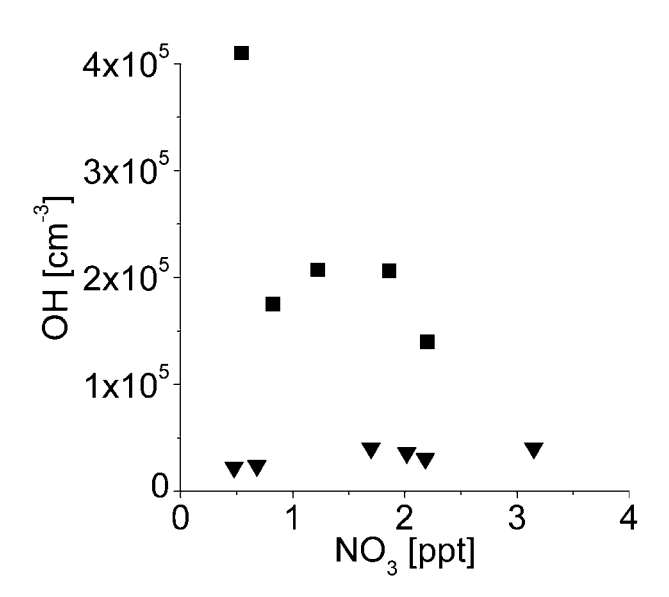


Figure 11. Correlation of the modeled concentration of OH and the mixing ratio of NO₃ for the nights 20 and 21 July (squares) and 4 and 5 August (triangles) during the BERLIOZ campaign.

 $10^5~{\rm cm}^{-3}~{\rm s}^{-1}$ are obtained. The mean nighttime oxidation capacity of OH of $1.3\times10^5~{\rm cm}^{-3}~{\rm s}^{-1}$ corresponds to 15% of the oxidation capacity of NO₃ during night, which ranged from 1.1×10^5 to $59\times10^5~{\rm cm}^{-3}~{\rm s}^{-1}$ [compare to *Geyer et al.*, 2001]. On a 24 hour basis the contribution of modeled nighttime OH to the total atmospheric oxidation capacity (VOCs, CO, and CH₄) was found to be 2.6% (the contribution of NO₃ to the diurnally integrated oxidation capacity was 17%) [*Geyer et al.*, 2001]. Note that the mean measured nighttime OH concentration is a factor 6 lower than the modeled one (cf. discussion in section 4.4). The contribution of measured nighttime OH to the oxidation processes in the atmosphere should therefore be less than 0.5% and can be neglected compared to other oxidants.

6. Conclusion

- [41] In the framework of the BERLIOZ campaign, intensive measurements of boundary layer concentrations of free radicals and a large number of ancillary species were performed in July/August 1998 at the semipolluted rural site of Pabstthum, near Berlin. Simultaneous observations of NO_3 , RO_2 , HO_2 , and OH took place during several nights producing one of the most comprehensive data sets of nighttime radical measurements. A box model was developed to study the role of NO_3 and other trace gases for the observed nighttime concentrations of RO_x . Following conclusions for nighttime production of peroxy and hydroxyl radicals can be drawn from the Pabstthum data set:
- 1. Nighttime mixing ratios of NO_3 , RO_2 , and HO_2 up to 70, 22, and 4 ppt, respectively, were measured during the campaign. The OH concentration reached (1.85 \pm 0.82) \times 10^5 cm⁻³ (averaged over 20 min) during one night but remained below the detection limit during the other nights.
- 2. Model results and ambient observations of RO_2 and HO_2 are in good agreement. Modeled RO_2 mixing ratios reached 40 ppt. HO_2 mixing ratios up to 6 ppt were modeled. In one night the model yielded an OH level of (4.1 \pm 0.7) \times 10⁵ cm⁻³ while (1.60 \pm 0.85) \times 10⁵ cm⁻³ were measured. This overestimation by the model could point to a missing nocturnal sink of OH. For the rest of the nights the modeled concentrations of OH are just within the upper limit of the measurements.
- 3. Reactions of NO_3 with VOCs, mainly with biogenic monoterpenes, were shown to constitute a considerable source of organic peroxy radicals during nighttime. The contribution of NO_3 to nighttime RO_2 production averaged to 77% during the campaign. NO_3 was responsible for 53% of the HO_2 and 36% of the OH radicals measured during night. Ozonolysis of alkenes formed 12% of the RO_2 , 47% of the RO_2 and 64% of the OH radicals during night. Another 11% of the RO_2 radicals were formed by OH–VOC reactions.
- 4. Generally a positive linear correlation of the mixing ratios of RO₂ and NO₃ was observed and modeled during the campaign. The analysis shows that this dependence can be attributed to the role of NO as a sink for both radicals, which are depleted efficiently at increasing NO levels. In addition during nights with VOCs were of minor importance for the NO₃ removal, the production rate of RO₂ increased with increasing NO₃ concentration. The results of Pabstthum were compared to former simultaneous measurements of

- RO₂ and NO₃ by *Mihelcic et al.* [1993] and *Carslaw et al.* [1997]. In contrast to the semipolluted site Pabstthum a negative correlation between RO₂ and NO₃ can arise under conditions, which are typical for a clean, forested site.
- 5. During many nights a rapid increase of the RO_x mixing ratio was observed after sunset followed by a maximum of some hours length before it slowly decreased again. This profile of RO_x is also predicted by the model and can be attributed to the positive dependence of RO_2 to NO_3 and the observed nighttime profile of NO_3 showing the same trend as the RO_2 mixing ratio.
- 6. The correlation of OH and NO₃ was found to be an indicator for the contribution of NO₃ to nighttime OH production: While a negative correlation appeared during nights with ozonolysis dominating the OH production, OH was weakly positively correlated during nights when reactions of NO₃ with VOC were of major importance.
- 7. The contribution of OH to the nocturnal oxidation capacity of the atmosphere (with respect to VOCs, CO, and CH₄) was modeled for the situation at Pabstthum (semi polluted rural environment, high values of biogenic VOCs, nighttime NO_2 around 5 ppb, O_3 around 40 ppb) to have been 15% of that of NO_3 corresponding to a contribution of 2.6% to the 24 hour integral of the total atmospheric oxidation capacity. With respect to the factor 6 between modeled and measured OH levels the contribution should be less than 0.5% and therefore negligible.
- [42] **Acknowledgments.** This project was supported by the BMBF in the framework of TFS-LT3 (contract 422-4007-07TFS 31/H.B.3).

References

- Alicke, B., A. Geyer, A. Hofzumahaus, F. Holland, S. Konrad, H. W. Pätz, J. Schäfer, J. Stutz, A. Volz-Thomas, and U. Platt, OH formation by HONO photolysis during the BERLIOZ experiment, *J. Geophy. Res.*, 108(D4), doi:1029/2001JD000579, in press, 2003.
- Ariya, P. A., R. Sander, and P. J. Crutzen, Significance of HO_x and peroxides production due to alkene ozonolysis during fall and winter: A modeling study, *J. Geophys. Res.*, 105, 17,721–17,739, 2000.
- Atkinson, R., Gas-phase tropospheric chemistry of volatile organic compounds, 1, Alkanes and alkenes, J. Phys. Chem. Ref. Data, 26, 215–290, 1997.
- Atkinson, R., Atmospheric chemistry of VOCs and NO_x, Atmos. Environ., 34, 2063-2101, 2000.
- Atkinson, R., E. S. C. Kwok, J. Arey, and S. M. Aschmann, Reactions of alkoxy radicals in the atmosphere, *Faraday Discuss.*, 100, 23–37, 1995.
 Atkinson, R., D. L. Baulch, R. A. Cox, R. F. Hampson, J. A. Kerr Jr., M. J. Rossi, and J. Troe, Evaluated kinetic, photochemical and heterogeneous data for atmospheric chemistry: Supplement V, J. Phys. Chem. Ref. Data, 26, 521–1011, 1997.
- Benter, T., M. Liesner, R. N. Schindler, J. Hjorth, and G. Restelli, REMPI-MS and FTIR study of NO₂ and oxirane formation in the reactions of unsaturated hydrocarbons with NO₃ radicals, *J. Phys. Chem.*, *98*, 10,492–10,496, 1994.
- Bey, I., B. Aumont, and G. Toupance, The nighttime production of OH radicals in the continental troposphere, *Geophys. Res. Lett.*, 24, 1067–1070, 1997
- Bey, I., B. Aumont, and G. Toupance, A modelling study of the nighttime radical chemistry in the lower continental troposphere, 2, Origin and evolution of HOx, *J. Geophys. Res.*, 106, 9991–10,001, 2001.
- Canosa-Mas, C. E., P. S. Monks, and R. P. Wayne, Temperature dependence of the reaction of the nitrate radical with but-1-ene, *J. Chem. Soc. Faraday Trans.*, 88, 11–14, 1992.
- Cantrell, C. A., R. E. Shetter, J. G. Calvert, F. L. Eisele, and D. J. Tanner, Some considerations of the origin of nighttime peroxy radicals observed in MILOPEX 2c, *J. Geophys. Res.*, 102, 15,899–15,913, 1997.
- Carslaw, N., L. J. Carpenter, J. M. C. Plane, B. J. Allan, R. A. Burgess, K. C. Clemitshaw, H. Coe, and S. A. Penkett, Simultaneous observations of nitrate and peroxy radicals in the marine boundary layer, *J. Geophys. Res.*, 102, 18,917–18,933, 1997.

- Clemitshaw, K. C., L. J. Carpenter, S. A. Penkett, and M. E. Jenkin, A calibrated radical chemical amplifier for ground-based tropospheric measurements, J. Geophys. Res., 102, 25,405-25,416, 1997
- DeMore, W. B., S. P. Sander, C. J. Howard, A. R. Ravishankara, D. M. Golden, C. E. Kolb, R. F. Hampson, M. J. Kurylo, and M. J. Molina, Chemical Kinetics and Photochemical Data for Use in Stratospheric Modeling, Evaluation Number 12, JPL Publ. 97-4, NASA, 1997.
- Eisele, F. L., D. J. Tanner, C. A. Cantrell, and J. G. Calvert, Measurements and steady state calculations of OH concentrations at Mauna Loa Observatory, J. Geophys. Res., 101, 14,665-14,680, 1996.
- Geyer, A., B. Alicke, D. Mihelcic, J. Stutz, and U. Platt, Comparison of tropospheric NO₃ radical measurements by differential optical absorption spectroscopy and matrix isolation electron spin resonance, J. Geophys. Res., 104, 26,097, 1999.
- Geyer, A., B. Alicke, S. Konrad, J. Stutz, and U. Platt, Chemistry and oxidation capacity of the nitrate radical in the continental boundary layer near Berlin, J. Geophys. Res., 106, 8013-8025, 2001.
- Gölz, C., J. Senzig, and U. Platt, NO3-initiated oxidation of biogenic hydrocarbons, Chemosphere Global Change Sci., 3(3), 339-352, 2001.
- Grenfell, J. L., et al., Tropospheric box-modelling and analytical studies of the hydroxyl (OH) radical and related species: Comparison with observations, J. Atmos. Chem., 33, 183-214, 1999.
- Grossmann, D., et al., Hydrogen peroxide, organic peroxides, carbonyl compounds, and organic acids measured at Pabstthum during BERLIOZ, J. Geophys. Res., 108(D4), doi:10.1029/2001JD001096, in press, 2003.
- Guenther, A., C. Geron, T. Pierce, B. Lamb, P. Harley, and R. Fall, Natural emissions of non-methane volatile organic compounds, carbon monoxide, and oxides of nitrogen from North America, Atmos. Environ., 34, 2205-2230, 2000.
- Hakola, H., J. Arey, S. Aschmann, and R. Atkinson, Product formation from gas-phase reactions of OH radicals and O3 with a series of monoterpenes, J. Atmos. Chem., 18, 75-102, 1994.
- Heikes, B. G., and A. M. Thompson, Effects of heterogeneous processes on NO₃, HONO and HNO₃ chemistry in the troposphere, J. Geophys. Res., 88, 10,883-10,895, 1983.
- Hein, R., P. J. Crutzen, and M. Heimann, An inverse modeling approach to investigate the global atmospheric methane cycle, Global Biogeochem. Cycles, 11, 43-76, 1997.
- Heintz, F., H. Flentje, R. Dubois, and U. Platt, Long-term observation of nitrate radicals at the Tor Station, Kap Arkona (Rügen), J. Geophys. Res., 101, 22,891-22,910, 1996.
- Holland, F., U. Aschmutat, M. Heßling, A. Hofzumahaus, and D. H. Ehhalt, Highly time resolved measurements of OH during POPCORN using laserinduced fluorescence spectroscopy, J. Atmos. Chem., 31, 205-225, 1998.
- Holland, F., A. Hofzumahaus, J. Schäfer, A. Kraus, and H.-W. Pätz, Measurements of OH and HO₂ radical concentrations and photolysis frequencies during BERLIOZ, *J. Geophys. Res.*, 108(D4), 8246, doi:10.1029/2001JD001393, 2003.
- Hu, J. H., and J. P. D. Abbatt, Reaction probabilities for N2O5 hydrolysis on sulfuric acid and ammonium sulfate aerosols at room temperatures, J. Phys. Chem., 101, 871, 1997.
- Jacob, D. J., Heterogeneous chemistry and tropospheric ozone, Atmos. Environ., 34, 2131-2159, 2000.
- Janson, R. W., Monoterpene emissions from Scots pine and Norwegian spruce, J. Geophys. Res., 98, 2839-2850, 1993.
- Jenkin, M. E., S. M. Saunders, and M. J. Pilling, The tropospheric degradation of volatile organic compounds: A protocol for mechanism development, Atmos. Environ., 31, 31, 1997
- Jenkin, M. E., G. D. Hayman, R. G. Derwent, S. M. Saunders, N. Carslaw, S. Pascoe, and M. J. Pilling, Tropospheric chemistry modelling: Improvements to current models and application to policy issues, Rep. AEAT-4867/20150/R004, 1999.
- Jensen, N. R., J. Hjorth, C. Lohse, H. Skov, and G. Restelli, Products and mechanism of the gas-phase reactions of NO₃ with CH₃SCH₃, CD₃SCD₃, CH₃SH and CH₃SSCH₃, *J. Atmos. Chem.*, *14*, 95–108, 1992. Kanaya, Y., Y. Sadanaga, J. Matsumoto, U. K. Sharma, J. Hirokawa,
- Y. Kajii, and H. Akimoto, Nighttime observation of the HO2 radical by an LIF instrument at Oki island, Japan, and its possible origin, Geophys. Res. Lett., 26, 2179-2182, 1999.
- Konrad, S., et al., Hydrocarbons measurements at Pabstthum during the BERLIOZ campaign and modeling of free radicals, J. Geophys. Res., 108(D4), doi:10.1029/2001JD000866, in press, 2003.
- Kurtenbach, R., R. Ackermann, K. H. Becker, A. Geyer, J. A. G. Gomes, J. C. Lörzer, U. Platt, and P. Wiesen, Verification of the contribution of

- vehicular traffic to the total NMVOC emissions in Germany and the importance of the NO₃ chemistry in the city air, J. Atmos. Chem., 42, 395-411, 2002.
- Le Bras, G., C. Gölz, and U. Platt, Production of peroxy radicals in the DMS oxidation during night-time, in Dimethylsulphide, Oceans, Atmosphere and Climate, Proceedings of the International Symposium, Belgirate, Italy, 13-15 October 1992, edited by G. Restelli and G. Angeletti, Kluwer Acad., Norwell, Mass., 1993.
- Lightfoot, P. D., R. A. Cox, J. N. Crowley, M. Destriau, G. D. Hayman, M. E. Jenkin, G. K. Moortgat, and F. Zabel, Organic peroxy radicals: Kinetics, spectroscopy and tropospheric chemistry, Atmos. Environ., 26, 1805-1961, 1992.
- Martinez, E., B. Cabanas, A. Aranda, P. Martin, and S. Salgado, Absolute rate coefficients for the gas-phase reactions of NO3 radical with a series of monoterpenes at T = 298 to 433 K, J. Atmos. Chem., 33, 265-282, 1999.
- Mihelcic, D., D. Klemp, P. Müsgen, H. W. Pätz, and A. Volz-Thomas, Simultaneous measurements of peroxy and nitrate radicals at Schauinsland, J. Atmos. Chem., 16, 313-335, 1993.
- Mihelic, D., et al., Comparison of measurements and model calculation of OH- HO₂-, RO₂- radicals and local ozone production during the BER-LOIZ campaign, J. Geophys. Res., submitted manuscript, 2003.
- Paulson, S. E., and J. J. Orlando, The reactions of ozone with alkenes: An important source of HO_x in the boundary layer, Geophys. Res. Lett., 23, 3727-3730, 1996.
- Paulson, S. E., M. Y. Chung, and A. S. Hasson, OH radical formation from the gas-phase reaction of ozone with terminal alkenes and the relationship between structure and mechanism, J. Phys. Chem. A, 103, 8125-8138, 1999
- Placet, M., C. Mann, R. Gilbert, and M. Niefer, Emissions from stationary sources, Atmos. Environ., 34, 2183-2204, 2000.
- Platt, U., D. Perner, H. Schroeder, G. Kessler, and A. Toenissen, The diurnal variation of NO₃, J. Geophys. Res., 86, 11,965-11,970, 1981.
- Platt, U., The origin of nitrous and nitric acid in the atmosphere, in Chemistry of Multiphase Atmospheric Systems, edited by W. Jäschke, pp. 299-319, Springer-Verlag, New York, 1986.
- Platt, U., G. Le Bras, G. Poulet, J. P. Burrows, and G. K. Moortgat, Peroxy radicals from nighttime reaction of NO3 with organic compounds, Nature, 348, 147-149, 1990.
- Sawyer, R., R. Harley, S. Cadle, H. Bravo, R. Slott, R. Gorse, and J. Norbeck, Mobile sources, Atmos. Environ., 34, 2161-2181, 2000.
- Saylor, R. D., An estimate of the potential significance of heterogeneous loss to aerosols as an additional sink for hydroperoxy radicals in the troposphere, Atmos. Environ., 31, 3653-3658, 1997.
- Volz-Thomas, A., H.-W. Pätz, N. Houben, S. Konrad, D. Mihelcic, T. Klupfel, and D. Perner, Inorganic trace gases and peroxy radicals during BERLIOZ at Pabstthum: An investigation of the photostationary state of NO_x and O₃, J. Geophys. Res., 108(D4), doi:10.1029/2001JD001255, in press, 2003.
- Wängberg, I., I. Barnes, and K. H. Becker, Product and mechanistic study of the reaction of NO₃ radicals with α-pinene, Environ. Sci. Technol., 31, 2130-2135, 1997.
- Wayne, R. P., et al., The nitrate radical: Physics, chemistry, and the atmosphere, Atmos. Environ., 25A, 1-203, 1991.
- Wesley, M. L., and B. B. Hicks, A review of the current status of knowledge on dry deposition, Atmos. Environ., 34, 2261-2282, 2000.
- Wex, H., C. Neusüss, M. Wendiseh, F. Stratmann, C. Koziar, A. Keil, A. Wiedensohler, and M. Ebert, Particle scattering, backscattering, and absorption coefficients: An in situ closure and sensitivity study, J. Geophys. Res., 107(D21), 8122, doi:10.1029/2000JD000234, 2002.

K. Bächmann, Institut für Anorganische Chemie, TH Darmstadt, Darmstadt, Germany.

A. Geyer, Department of Atmospheric Sciences, University of California, 7172 Math Sciences, Box 95 1565, Los Angeles, CA 90095, USA.

A. Hofzumahaus, F. Holland, S. Konrad, D. Mihelcic, H.-W. Pätz, H.-J. Schäfer, and A. Volz-Thomas, Institut für Atmosphärische Chemie, Forschungszentrum Jülich, D-52425 Jülich, Germany.

T. Klüpfel and D. Perner, Max-Planck-Institut für Chemie, Mainz, Germany.

U. Platt, Institut für Umweltphysik, Universität Heidelberg, Im Neuenheimer Feld 229, D-69120 Heidelberg, Germany.

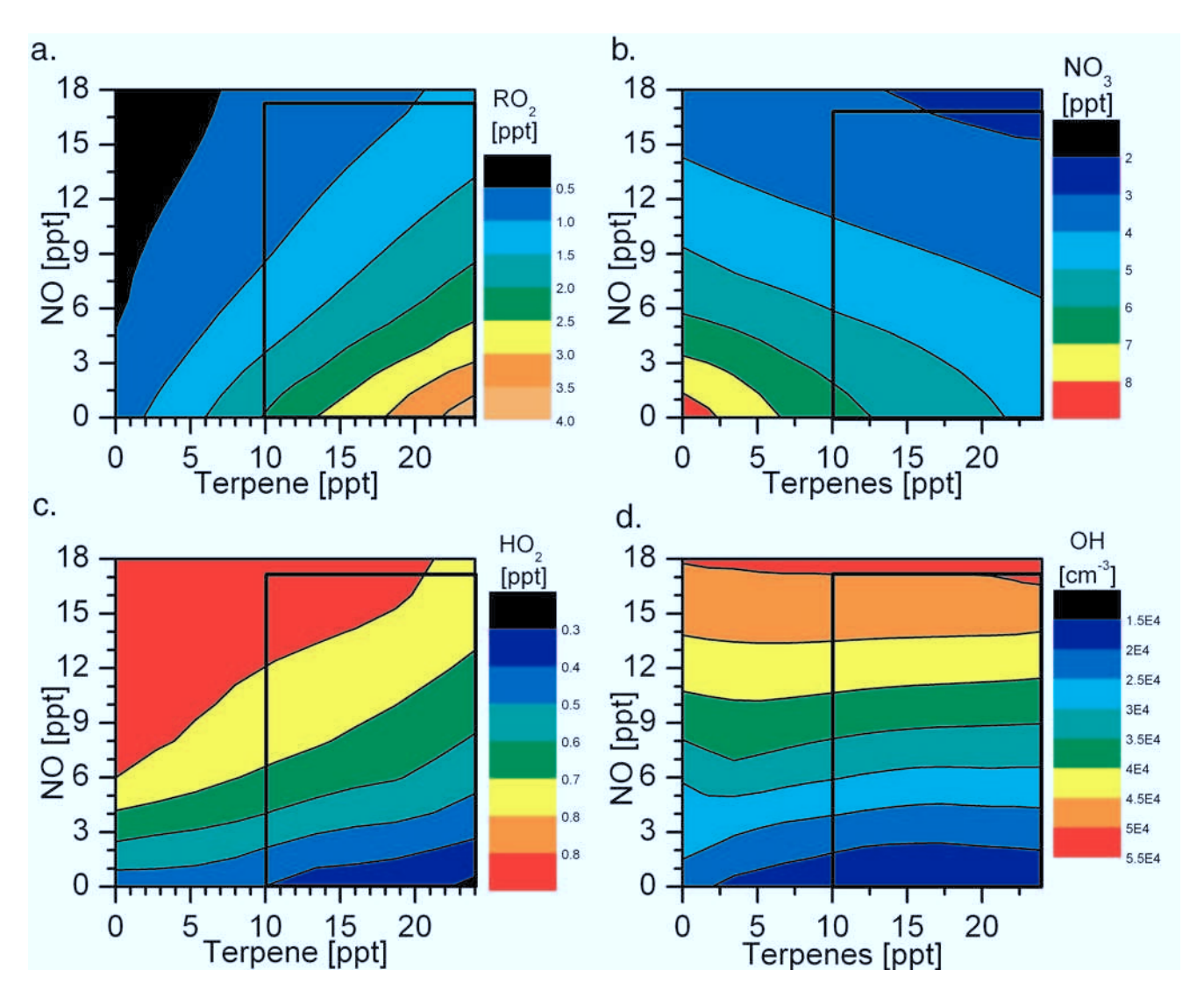


Figure 4. Sensitivity study of the modeled mixing ratios of RO₂ (a), NO₃ (b), and HO₂ (c) and the concentration of OH (d) on the mixing ratios of NO and monoterpenes for 4 August 1998, 2027 UT at Pabstthum, Germany.